COMMUNICATION

ChemComm
www.rsc.org/chemcomm

Thermostable sulfated 2–4 nm tetragonal ZrO_2 with high loading in nanotubes of SBA-15: a superior acidic catalytic material

M. V. Landau,*[a] L. Titelman,[a] L. Vradman[b] and P. Wilson[a]

[a] *Blechner Center for Industrial Catalysis and Process Development, Department of Chemical Engineering, Ben-Gurion University of the Negev, Beer-Sheva-84105, Israel. E-mail: mlandau@bgumail.bgu.ac.il*

[b] *Department of Chemical Engineering, Negev Academic College of Engineering, Beer-Sheva 84100, Israel*

Received (in Cambridge, UK) 26th November 2002, Accepted 9th January 2003
First published as an Advance Article on the web 3rd February 2003

The high-loaded (48–60 wt.%) 2–4 nm tetragonal ZrO_2 phase inserted in mesostructured silica SBA-15 by chemical solution decomposition (CSD) of Zr(n-PrO)$_4$ and activated at 873 K displayed ~3 times higher capacity for surface sulfate ions and, respectively, 1.5–2.2 times higher catalytic activity per gram of SO_4-ZrO_2/SBA-15 composite in condensation of MeOH with *t*-BuOH and dehydration of isopropanol compared with the regular bulk sulfated zirconia material.

Zirconia modified with sulfate anions forms a highly acidic catalytic phase with an excellent performance in a variety of acid-catalyzed reactions.[1,2] The highest acidity and catalytic activity displays a sulfated zirconia (SZ) material prepared by treatment with H_2SO_4 or $(NH_4)_2SO_4$ of dried $Zr(OH)_4$ gelated by ammonia from an aqueous solution of $ZrOCl_2$ or $ZrO(NO_3)_2$, followed by calcination in air at 873 K.[1,3,4] The material contains 2–3 S atoms nm^{-2} (1.2–1.5 wt% S),[4,5] zirconia in a tetragonal (T) modification.[6,7] and has a surface area of about 100 m^2 g^{-1} (crystal size ~10 nm).[1–7] Though the exact structure of the acid sites in this material is still a matter of debate[2] it is widely accepted that they are created by SO_4^{2-} anions adsorbed at the zirconia surface and their concentration should be inversely proportional to the ZrO_2-T crystal size. Therefore stabilizing the SZ catalytic phase with high sulfur retention ability within the pores of mesostructured silicas (MS) yielding a combination of high loading (≥50 wt%) and low crystal size (≤5 nm) of T-zirconia phase should give a superior acidic catalyst.

Several attempts to prepare the SZ/MS composites gave catalysts with higher activity of supported SZ phase but equal or lower activity per gram of catalyst compared with the bulk material.[8–11] This could be a result of location of the part of zirconia phase as large crystals outside of MS channels or as a grafted amorphous layer. We adopted the CSD method[12] to locate the small Zr-phase nanocrystals exclusively inside the nanotubes of hexagonal MS SBA-15 controlling the crystallinity of ZrO_2-T phase. 3 g of SBA-15 MS synthesized according[13] to which texture characteristics are presented in Table 1, was impregnated with a 70 wt% solution of Zr(n-PrO)$_4$ in *n*-propanol (Aldrich). After separation the excess of solution by filtration the wet solid in a 100 cm^3 glass was placed in an 1 L autoclave that contained 180 cm^3 of pure *n*-propanol. The CSD was conducted for 3 h at 493 K (5 K min^{-1}). After cooling and discharging the solid was dried under vacuum at 473 K for 2 h. The CSD of Zr(n-PrO)$_4$ occurred inside the channels of SBA-15 because the evaporation of the solvent and pulling out the Zr-solution by capillary forces was prevented by *n*-propanol saturated pressure outside the pores. It yielded a highly dispersed Zr-oxide phase at 48 wt%ZrO_2 loading (EDX, JEOL JEM-5600 microscope). The wide reflections in the X-ray diffractogram (Philips PW 1050/70, CuK_α) at 2θ ~30, 50 and 60° were evident for formation of small <2 nm particles with a short range order close to ZrO_2-T. After calcination in air at 773–873 K XRD detected a growth of particle size to 4.5 nm (Sherrer equation, API Philips software) and appearance of all the reflections characteristic for a ZrO_2-T phase. Formation of ZrO_2-T 3–5 nm nanoparticles in the nanotubular channels of calcined ZrO_2-SBA-15 was detected also by HRTEM (JEOL Fas JEM 2010 microscope). All the EDX data collected with an electronic spot 25 nm from different points of the ZrO_2-SBA-15 composite gave similar Zr contents. No particles of pure ZrO_2 with the shape other than fiber-like packages of silica nanotubes characteristic for parent SBA-15 were detected in the composite material by SEM-mapping. Similar information was collected for a composite prepared by repeating the CSD procedure for 48 wt%ZrO_2/SBA-15 sample yielding a material with 60 wt% ZrO_2 content. The amounts of crystalline ZrO_2-T phase in the composite samples calcined at 873 K were calculated based on the integral intensities of the XRD peaks corresponding to zirconia, silica phases and calibration data. They were close to the content of ZrO_2 calculated according to the elemental composition. Conducting the CSD of Zr(PrO)$_4$ according to ref. 12 in the absence of SBA-15 yielded the ZrO_2(T) phase with a crystal size of 15 nm (XRD) after calcination at 873 K. It indicates the high thermostability of the ZrO_2 nanophase embedded in nanotubular channels of SBA-15.

The dried ZrO_2-SBA-15 composites were treated with 0.5 M aqueous H_2SO_4 at S:Zr ratios of 0.1–2.0. The slurry was evaporated on a plate at 313–323 K, dried in air at 373 K

Table 1 SO_4/ZrO_2/SBA-15 composites and reference bulk SO_4/ZrO_2 catalysts: properties and performance

Sample	ZrO_2 phase (tetragonal)				Texture parameters			Sulfur content		Catalytic performance		
	Content/wt%		Crystal size/nm		SA/m^2 g^{-1}	PV/cm^3 g^{-1}	PD/ nm	wt%	S/Zr	Reaction I	Reaction II	
	EDAX	XRD	XRD	HRTEM						MTBE Yield, %	X_2 %	S_2 %
SBA-15	—	—	—	—	847	1.3	6.7	—	—	—	—	—
SO_4/ZrO_2	97.2	—	11	—	92	0.08	3.4	1.08	0.037	20.1	5.8	82.3
SO_4/ZrO_2 (MEL, x20 1077/01)	96.8	—	10	—	107	0.09	3.4	1.18	0.043	22.6	6.2	83.0
SO_4/48% ZrO_2/SBA	48.1	47	3.5	2.5–4.0	405	0.49	3.7	1.79	0.16	32.3	9.2	84.5
SO_4/60% ZrO_2/SBA	59.8	58	3.5	2.5–4.5	280	0.25	3.6	2.20	0.15	46.2	13.2	85.0

X_2—Iso—PrOH conversion. S_2—Diisopropyl ether selectivity.

DOI: 10.1039/b211585a

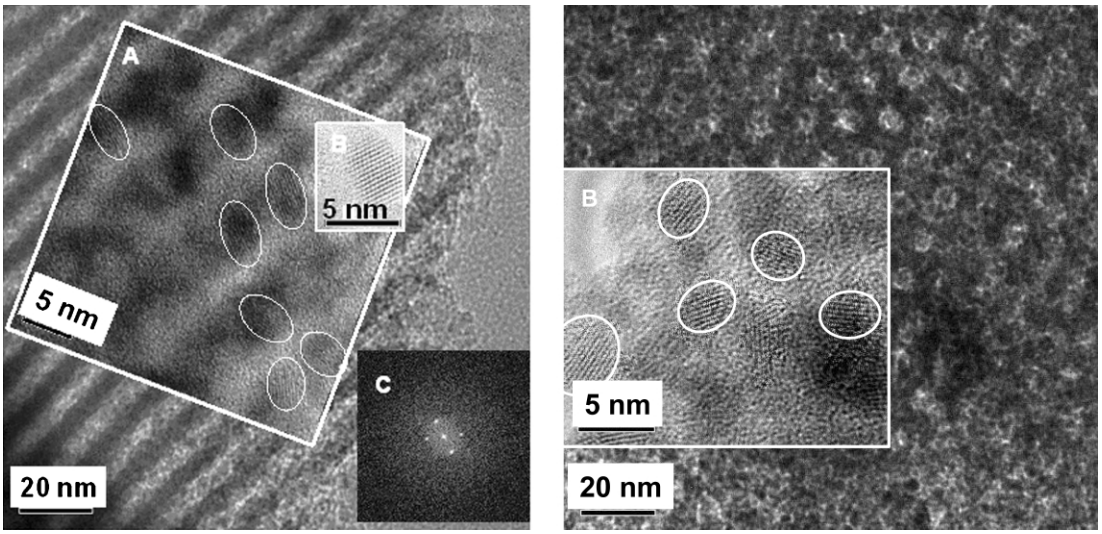

Fig. 1 HRTEM micrographs and images of sulfated ZrO_2 nanocrystals embedded in nanotubes of SBA—15 mesoporous silica in sample $SO_4/60\%ZrO_2$/SBA: left—side view; right—front view (channel entrances).

overnight and calcined at 873 K for 3 h (heating rate 15 K min^{-1}).The content of the ZrO_2-T phase (crystal size ~3.5 nm) detected in calcined supported SZ by XRD was equal to its potential content (EDX) up to the S:Zr in the initial slurry = 0.3. It yielded a S:Zr ratio of = 0.15 in calcined SZ-SBA-15 composites. At higher initial S:Zr ratios the crystallinity of the calcined zirconia phase decreased due to formation of $Zr(SO_4)_2$ being 60 and 12% at S:Zr = 1.0 and 2.0, respectively. The reference SZ was prepared according to ref. 3, starting from $ZrOCl_2$ with the final calcination temperature of 873 K. The material contained ZrO_2(T) phase having a crystal size of ~11 nm (XRD) and S:Zr ratio of 0.037 (Table 1). Similar characteristics figures were displayed by the commercial SZ sample (Table 1). The maximal S:Zr ratio obtained in calcined SZ-SBA-15 composites at 100% ZrO_2-T crystallinity was ~3 times higher than in bulk SZ samples being inversely proportional to the crystal size of ZrO_2(T)-phase.

At this optimal S:Zr ratio the SZ-phase was uniformly distributed inside the nanotubes of SBA-15 as 2–4 nm nanoparticles (Fig. 1) leaving ~3.5 nm mesopores and surface area of 280–405 $m^2\ g^{-1}$ depending on Zr-loading (Table 1). The high values (0.83–0.92) of normalized surface area calculated for calcined SZ-SBA-15 composites,[14] indicate minimal pore blocking of parent MS. Parallel fringes across the nanoparticle images in the insets A,B of Fig. 1 have a periodicity of 3.0 Å which corresponds to planes (101) with *d*-spacings equal to d_{101} = 3.00 Å in tetragonal ZrO_2 structure. An electron diffraction pattern at the inset C (Fig. 1) exhibits a set of diffraction spots which could be indexed on the basis of unit cell parameters of ZrO_2-T phase.

The amount of sulfur species adsorbed by zirconia nanocrystals embedded in SBA-15 at 100% ZrO_2(T) crystallinity was 3 times higher than in a regular bulk SZ (Table 1). Assuming them to be acid sites-creative species one could expect a 1.5–2 times higher acidity of optimized SZ-SBA-15 composites with 48–60 wt% ZrO_2 loading relative to the bulk SZ. TPD (AMI-100,Zeton-Altamira) detected 1.5–2.1 times higher the amount of NH_3 desorbed from ZrO_2-SBA-15 at 393–1073 K after saturation at 313 K compared with that desorbed from reference SZ samples.

The catalysis tests were performed in a 50 cm^3 batch reactor at conditions where no transport limitations affected the reactions rates. This was proven by the linear dependence of substrate conversion on the catalysts loading (mg ml^{-1} reagents).

Table 1 presents the testing results for bulk and supported SZ catalysts optimized according to the sulfur content at 100% crystallinity of ZrO_2(T) phase. The performance evaluation was carried out in two selected acid-catalyzed reactions generally used for characterization of SZ performance: condensation of *t*-BuOH and MeOH (Reaction 1)† and dehydration of iso-PrOH (Reaction 2).† As expected, the activity of SZ-SBA-15 composites was 1.5–2.2 times higher compared with bulk SZ. The proportionality of substrate conversions to the catalysts sulfur content and similar selectivities to MTBE (100%) and diisopropyl ether measured with supported and bulk SZ are evident for the same nature of acid sites in the both the bulk and supported systems. Increasing the sulfur content in calcined SZ-SBA-15 composite beyond the optimal S:Zr value of ~0.15 caused a substantial drop of catalytic activity due to decreased crystallinity of ZrO_2(T) phase.

This research was supported by the Israel Academy of Sciences and Humanities. The authors thank to Mr V.Ezersky for conducting the HRTEM measurements.

Notes and references

† Reaction 1 was conducted at 398 K, MeOH/*t*-$BuOH_{mol}$ = 2.4, τ = 2 h, catalysts loading 8.9 mg ml^{-1}; Reaction 2—at 473 K, τ = 2 h, catalysts loading 3 mg ml^{-1}.

1 K. Arata, *Adv.Catal*., 1990, **37**, 165.
2 G. D. Yadav and J. J. Nair, *Micropor. Mesopor. Mater*., 1999, **33**, 1.
3 M. Hino and K. Arata, *J. Chem. Soc., Chem. Commun*., 1980, 851.
4 N. Katada, J. Endo, K. Notsu, N. Yasunobu, N. Naito and M. Niwa, *J. Phys. Chem, B*, 2000, **104**, 10321.
5 P. Nascimento, C. Akratopoulou, M. Oszagyan, G. Coudurier, C. Travers, J. F. Jolu and J. C. Vedrdine, *Stud. Surf. Sci. Catal*., 1992, **75**, 1185.
6 C. Morterra, G. Cerrati, F. Pinna and M. Signoretto, *J. Catal*., 1995, **157**, 109.
7 C. R. Vera, . L. Pieck, K. Shimizu and J. M. Parera, *Appl. Catal. A*, 2002, **230**, 137.
8 Q.-H. Xia, K. Hidajat and S. Kawi, *Chem. Commun*, 2000, 229 (*J. Catal*., 2002, **205**, 318).
9 W. Hua, Y. Yue and Z. Gao, *J. Mol. Catal. A. Chem*., 2001, **170**, 195.
10 H. Matsuhashi, M. Tanaka, H. Nakamura and K. Arata, *Appl. Catal. A*, 2001, **208**, 1.
11 Y. Sun, L. Zhu, H. Lu, R. Wang, S. Lin, D. Jiang and F.-S. Xiao, *Appl. Catal. A*, 2002, **237**, 21.
12 M. Inoue, H. Kominami and T. Inui, *Appl. Catal. A*, 1993, **97**, L25.
13 13. Zhao, J. Sun. Q. Li and G. D. Stucky, *Chem. Mater*., 2000, **12**, 275.
14 14. M. V. Landau, L. Vradman, M. Herskowitz, Y. Koltypin and A. Gedanken, *J. Catal*., 2001, **201**, 22.